How to Cite: Kareem, D.W., & Ways, T.M. (2026). Comparative Development and Characterization of Itraconazole-Loaded Solid Lipid Nanoparticles Incorporating Myristic Acid and Pluronic F127 for Oral Delivery. *Eurasian Journal of Chemistry, 31, 1(121), 100–120.* https://doi.org/10.31489/2959-0663/1-26-11

Article

Received: 13 December 2025 | Revised: 03 March 2026 | Accepted: 10 March 2026 | Published online: 17 March 2026

UDC 541.1; 66.095.2

https://doi.org/10.31489/2959-0663/1-26-11

Darya Wahhab Kareem, Twana Mohammed M. Ways*

Department of Pharmaceutics, College of Pharmacy, University of Sulaimani, Sulaymaniyah, Iraq
*(*Corresponding author's e-mail: twana.mohammed@univsul.edu.iq)*

Comparative Development and Characterization of Itraconazole-Loaded Solid Lipid Nanoparticles Incorporating Myristic Acid and Pluronic F127 for Oral Delivery

This study developed itraconazole-loaded solid lipid nanoparticles (SLNs) to enhance the solubility of this poorly water-soluble antifungal drug and evaluate key physicochemical properties. SLNs were prepared using the microemulsion technique with solid lipids stearic acid, palmitic acid, and myristic acid, and surfactants Tween 80 and Pluronic F127. The synthesized SLNs were characterized using dynamic light scattering (DLS) and electrophoretic light scattering (ELS) for size and zeta potential determination, while transmission electron microscopy (TEM) and field emission scanning electron microscopy (FESEM) were employed to examine surface morphology. Furthermore, the structural and thermal properties of the formulation were analyzed via Fourier transform infrared (FTIR) spectroscopy, X-ray diffraction (XRD), and differential scanning calorimetry (DSC). Among the formulations, SLN3 (containing stearic acid–Pluronic F127) and SLN9 (containing myristic acid–Tween 80) exhibited the smallest particle sizes and lowest polydispersity indices. Encapsulation efficiency was 97.04 ± 0.004 % for SLN3 and 42.69 ± 0.02 % for SLN9, with drug loading capacities of 3 ± 0.1 % and 1.8 ± 0.17 %, and yields of 50.03 ± 3.55 % and 57.9 ± 6.6 %, respectively. Solubility of ITZ increased to 2900 µg/mL (SLN3) and 3369 µg/mL (SLN9). *In vitro* release studies demonstrated controlled and sustained drug release, with SLNs exhibiting formulation- and pH-dependent behavior; SLN3 provided more prolonged release under acidic conditions, whereas SLN9 showed relatively higher release at intestinal pH, reflecting differences in lipid chain length and surfactant type. These results indicate that the optimized SLNs improve ITZ solubility and exhibit favorable physicochemical characteristics, supporting their potential as oral delivery systems for poorly soluble antifungal agents.

Keywords: itraconazole, solid lipid nanoparticles, solubility enhancement, stearic acid, myristic acid, Pluronic F127, Tween 80, controlled drug release

Introduction

Itraconazole (ITZ) is a triazole antifungal agent with a broad spectrum of activity against a wide range of dermal and systemic fungal infections. It is commonly prescribed for both immunocompromised and non-immunocompromised patients and is often preferred in cases where amphotericin B therapy is contraindicated due to its comparatively favorable safety profile [1]. Despite its clinical efficacy, the therapeutic performance of ITZ following oral administration is limited by significant formulation-related challenges [2]. One major limitation of ITZ is its poor aqueous solubility, which results from its highly lipophilic nature. Accordingly, ITZ is classified as a Biopharmaceutics Classification System (BCS) class II drug, characterized by low solubility and high membrane permeability. This poor solubility leads to slow and incomplete dissolution in gastrointestinal fluids, contributing to low and highly variable oral bioavailability among patients. [3]. In addition to solubility-related issues, uncontrolled or rapid drug release from certain oral formulations may result in high peak plasma concentrations, which have been associated with concentration-dependent adverse effects, including hepatotoxicity, elevations in hepatic enzymes and cardiotoxicity. ITZ is a potent inhibitor of cytochrome P450 3A4 (CYP3A4), and concomitant use with other CYP3A4 substrates can lead to elevated plasma concentrations of co-administered drugs, significantly increasing the risk of serious toxicities including QT prolongation [4]. Thus, while enhancing solubility is necessary to improve oral absorption, excessive or rapid release of ITZ can increase the risk of systemic toxicity. Therefore, an optimal oral formulation should not only improve solubility and dissolution but also provide controlled drug release to maintain plasma concentrations within the therapeutic window [5]. Therefore, the development of novel delivery systems with features such as reduced particle size, protection of the drug from degradation, improved drug solubility and the ability to provide sustained drug release is essential for the successful administration of ITZ. Nanoparticulate drug delivery systems have emerged as promising approaches to overcome the limitations

associated with conventional formulations. Example includes solid lipid nanoparticles (SLNs), colloidal carriers with particle size ranging from 50–1000 nm, first developed at the beginning of 1990s [6]. SLNs-based formulations have since been investigated for several routes of administration, including parenteral, oral, ocular, pulmonary, and rectal [7]. SLNs have attracted considerable attention as a potential drug carrier as they offer many advantages compared to other carrier systems. Compared with polymeric nanoparticles, SLNs are generally prepared from physiological lipids, which are biodegradable and biocompatible, reducing concerns of long-term toxicity [8]. Unlike liposomes, SLNs exhibit greater physical stability and lower risk of rapid leakage of incorporated drug [9]. Compared with nanoemulsions, SLNs are typically composed of solid lipids (e.g., fatty acids, waxes, or triglycerides) stabilized with surfactants and co-surfactants. The solid lipid matrix can improve drug stability, which in some cases, enables sustained or controlled drug release [10]. Despite the advantages of SLNs, ITZ has not been comprehensively investigated in such formulations. Previous attempts have largely been limited to general SLN systems without systematic evaluation of lipid type and surfactant composition. Although previous studies focused on topical and ocular delivery of ITZ-loaded SLNs, their potential for oral delivery has not been explored [11]. In particular, there is a lack of detailed studies examining the effects of different long-chain fatty acids such as stearic acid, palmitic acid, and myristic acid as lipid matrices, in combination with surfactants like Tween 80 and Pluronic F127, on the physicochemical properties, the solubility of ITZ, and release behavior of ITZ-loaded SLNs. This gap limits the ability to optimize formulations for enhanced solubility and stability of ITZ-loaded SLNs. Although Mukherjee et al. [12] demonstrated the feasibility of encapsulating ITZ into SLNs using palmitic acid as the lipid matrix and a combination of Pluronic F127 and Tween 80 as surfactants, systematic studies exploring alternative lipid matrices and surfactant systems for ITZ-loaded nanoparticles remain limited. In this study, we report the formulation and characterization of ITZ-loaded SLNs prepared using stearic acid, palmitic acid, and myristic acid as lipid carriers, stabilized with Tween 80 and Pluronic F127. Stearic acid, palmitic acid, and myristic acid were selected as solid lipids based on their well-established safety, biocompatibility, and suitability for oral drug delivery [13]. These lipids are naturally occurring saturated fatty acids that are widely used as pharmaceutical excipients and are metabolized through normal lipid metabolic pathways [14]. The selected lipids possess melting points above physiological temperature, ensuring that the lipid matrix remains in the solid state after administration, which is essential for the structural integrity and controlled drug release behavior of SLNs. Additionally, their hydrophobic nature promotes efficient drug incorporation and contributes to high entrapment efficiency [15]. To the best of our knowledge, this is the first comprehensive study systematically comparing the influence of different lipid, surfactant and cosurfactant combinations on the physicochemical properties of the ITZ SLNs including the particle size, polydispersity index, zeta potential, entrapment efficiency, and in vitro drug release of ITZ-loaded SLNs. Additionally, although myristic acid offers a favorable melting point, biocompatibility, and the potential to form stable lipid matrices, its use as a lipid matrix in combination with Pluronic F127 as a nonionic surfactant in ITZ SLNs has not been reported previously. By addressing this gap, this study provides important insights into the rational design of lipid-based nanocarriers for enhancing the solubility, stability and controlled release behavior of ITZ.

Experimental

Materials

ITZ was purchased from Kemprotec Limited (UK). Stearic acid, palmitic acid, myristic acid, Pluronic F127 (MWt ≈ 12,600 g/mol) and Tween 80 were purchased from Sigma-Aldrich (UK). Dimethyl sulfoxide (DMSO) was purchased from BIOCHEM Chemopharma (France). All other chemicals were of analytical grade and were used as received.

Methods

Solubility of ITZ in Lipids

The solubility of ITZ in three lipids — stearic acid, palmitic acid, and myristic acid — was determined quantitatively using a lipid-addition method according to Kumar and Goindi [11] with some modifications. Briefly, 10 mg of pure ITZ was placed in a tube, and 200 mg of molten lipid was added under continuous stirring at 70–75 °C using a hotplate stirrer (IKA® RCT Basic, Germany). Additional portions of lipid were sequentially added with continuous stirring until the mixture became turbid, indicating saturation. The total weight of lipid required to completely solubilize ITZ was recorded. A fixed amount of ITZ (10 mg) was selected to allow comparative evaluation of the lipid solubilization capacity under standardized conditions. The

initial amount of molten lipid (200 mg) was chosen to ensure complete immersion and adequate mixing of the drug at elevated temperature. Additional lipid was incrementally added until turbidity was observed, indicating the solubility limit had been reached. Solubility was calculated based on the total mass of lipid required to dissolve the fixed amount of ITZ and was expressed as mg of drug per gram of lipid. All experiments were performed in triplicate to ensure reproducibility and accuracy.

Preparation of ITZ Loaded SLN

Blank and ITZ loaded SLNs were prepared by a microemulsion technique as described by Gasco (1997) [16] with some modifications. The composition of the formulations is shown in Table 2 and Table S1. Solid lipids (stearic acid, palmitic acid and myristic acid) were melted at 70–75 °C by placing the solid lipid in a beaker within a water bath. Then ITZ was added to the molten lipid and stirred using a magnetic stirrer at 800 rpm until the drug was dispersed in the molten lipid. Then, to prepare aqueous phase, the surfactant (Tween 80 or Pluronic F127) was added to 4 mL distilled water and stirred until completely dispersed or dissolved in distilled water at the same temperature as the lipid phase. Following the preparation of both phases, the hot aqueous phase was added to the hot lipid phase and stirred at 800 rpm until an optically transparent system (warm microemulsion) was obtained. The warm microemulsion was immediately dispersed in cold water (15 °C), under high-speed homogenization (Ultra-Turrax T25 basic, Germany) at 8000 rpm for 15 min to trigger the SLNs formation. The volume ratio of warm microemulsion to cold water was 1:20.

Table 1

Composition of ITZ loaded SLNs formulations

S. No.	ITZ, mg	Stearic acid, g	Palmitic acid, g	Myristic acid, g	Tween 80, %	Pluronic F127, %	Ethanol, mL	Distilled water, mL
SLN 1	25	1			1			4
SLN 2	25	1			1.5			4
SLN 3	25	1				1		4
SLN 4	25	1				1.5		4
SLN 5	25		1		1			4
SLN 6	25		1		1.5			4
SLN 7	25		1			1		4
SLN 8	25		1			1.5		4
SLN 9	25			1	1			4
SLN10	25			1	1.5			4
SLN11	25			1		1		4
SLN12	25			1		1.5		4
SLN13	25	1			1.5		0.5	4
SLN14	25		1		1.5		0.5	4
SLN15	25			1	1.5		0.5	4
SLN16	12.5	1			1.5		0.5	4
SLN17	25	0.5		0.5	1.5			4

Turbidimetric Analysis

The turbidity of the ITZ-SLNs dispersions was measured at room temperature using a UV/visible spectrophotometer (PharmaSpec, UV-1700, Japan) at a maximum wavelength (λ_{max}) of 600 nm. The turbidity was determined from the absorbance of the dispersions, with distilled water was used as a blank.

pH Analysis

The pH of all ITZ-SLNs formulations was measured using a calibrated digital pH meter (Eutech instrument pH 700, Singapore). The electrode was directly immersed in each SLN dispersion, and the pH value was recorded upon stabilization. Measurements were performed at ambient temperature, and each formulation was assessed in triplicate.

Size, Size Distribution and Zeta Potential

A Zetasizer Nano ZS (Malvern Instruments Ltd., UK) was used to determine the particle size and size distribution of the SLNs by dynamic light scattering (DLS), and zeta potential by the electrophoretic light scattering (ELS). The SLNs dispersions were diluted with distilled water at a 1:100 ratio. Particle size meas-

urements were performed at a constant scattering angle of 90° and a controlled temperature of 25 °C. Each sample was analyzed in triplicate, with a 60-second equilibration period preceding measurement, utilizing 12 μL quartz cuvettes. The polydispersity index (PDI), indicating the measure of the distribution of nanoparticle population (size distribution), was also determined. Zeta potential measurements were conducted utilizing a disposable cell packed with carbon-coated electrodes. The electrophoretic mobility data were transformed into zeta potential utilizing the Smoluchowski model (Fκa = 1.5).

Effects of SLNs on ITZ Solubility

After preparing and evaluating all ITZ-SLN formulations, SLN3 and SLN9 were determined to be the optimum formula based on particle size and PDI data acquired using DLS. To evaluate the effect of SLN encapsulation on the aqueous solubility of ITZ, the solubility of the chosen formulations was measured using the shake-flask method.

An excess amount of pure ITZ and ITZ-loaded SLNs (SLN3 and SLN9) was individually introduced to 0.1 M simulated gastric fluid (SGF, pH 1.2; consisted of NaCl and HCl) and 0.1 M phosphate-buffered saline (PBS, pH 6.8; formulated from NaOH and KH_2PO_4). Each sample was made in three replicates. The suspensions were agitated continuously at 100 rpm for 48 hours at ambient temperature to achieve equilibrium. Following incubation, the mixtures were subjected to filtration through a 0.22 μm syringe filter to eliminate undissolved drug/particles. The filtrates were spectrophotometrically examined at a wavelength of 265 nm utilizing a UV-Visible spectrophotometer (PharmaSpec, UV-1700, Japan). The concentration of ITZ in each sample was determined using a standard calibration curve established in ethanol and distilled water, spanning a concentration range of 0.78–100 μg/mL.

Determination of Yield, Encapsulation Efficiency (EE), and Loading Capacity (LC)

To precipitate the SLNs and separate them from free ITZ, samples of the optimized formulations were centrifuged for 1 hour using a (Maanlab, HC 02R, Sweden, at 25 °C and 15,000 rpm). The resultant precipitates were collected, moved to a round-bottom flask with a thin neck, and then lyophilized using a Biobase BK-FD10P freeze dryer (China). The lyophilized SLNs were then collected, weighed and stored for further studies. Then the yield, encapsulation efficiency and drug loading capacity of the nanoparticles were calculated as follows:

The yield of the NPs was calculated using equation (1):

$$\text{Yield}\ (\%) = \frac{\text{Weight of dried SLNs obtained}}{\text{Total weight of drug+lipid+surfactant used}} \times 100\,\%, \tag{1}$$

After collecting the precipitated SLNs, the supernatant obtained from centrifugation (15,000 rpm, 1 hour, 25 °C) was analyzed spectrophotometrically using a UV/visible spectrophotometer at 265 nm (PharmaSpec, UV-1700, Japan) to quantify the amount of free ITZ based on a calibration curve prepared in ethanol/water (0.78–100 μg/mL). The encapsulated ITZ was then determined indirectly by subtracting the free drug in the supernatant from the total drug initially added. Encapsulation efficiency (EE%) and drug loading (DL%) were subsequently calculated using Equations (2) and (3).

$$\text{EE}\,(\%) = \frac{\text{Total drug-Free drug}}{\text{Total drug}} \times 100\,\%, \tag{2}$$

$$\text{DL}\ (\%) = \frac{\text{Amount of drug encapsulated}}{\text{Total weight of SLNs}} \times 100\,\%. \tag{3}$$

Fourier Transform Infrared (FTIR) Spectroscopy

FTIR spectroscopy was conducted using a Shimadzu FTIR-8400S spectrometer (Shimadzu Corporation, Japan). The analysis was performed on the pure ITZ, stearic acid, myristic acid, SLN3 and SLN9. The materials were mixed with potassium bromide (KBr) pellets using a mortar and pestle and then compressed using a hydraulic press to form a transparent pellet. The FTIR spectra were collected over the wavenumber range of 4000-400 cm^{-1}, using 3 scans with a resolution of 2 cm^{-1}.

Transmission Electron Microscopy (TEM)

TEM was used to examine the morphology of the ITZ-loaded SLNs at a 100 kV accelerating voltage using a transmission electron microscope (Carl Zess_EM1OC, Germany). One drop of SLN dispersions was applied on a copper grid coated with carbon and allowed to dry at room temperature for one minute. The

sample was then stained with uranyl acetate solution and left to air dry. Then, TEM imaging was conducted, and the particle size was measured from the TEM images using ImageJ 1.54 g software. The size distribution graphs were plotted using OriginPro software (version 2018 SR1, b9.51.195, OriginLab Corporation, Northampton, MA, USA).

Field Emission Scanning Electron Microscopy (FESEM)

The shape and surface texture of the SLNs were studied using a scanning electron microscope (TESCAN MIRA3 FESEM, Brno, Czech Republic). One drop of the optimized SLN dispersion was placed on an aluminum stub (TAAB Laboratories Equipment, Aldermaston, UK) utilizing a double-sided sticky tab (TAAB Laboratories Equipment) and, following drying, was vacuum-coated with gold–palladium in an argon atmosphere for 60 seconds. Imaging was conducted at an accelerating voltage of 15 kV, with magnifications of between 5000× and 135,000×, and a working distance of 4.91 mm.

Powder X-Ray Diffraction (PXRD)

The X-ray diffraction patterns for ITZ, stearic acid, myristic acid, SLN3 and SLN9 were recorded using an X-ray diffractometer (Bruker, Model No: D8 advance, Germany). The investigation was conducted using a diffractometer with a Cu Kα radiation source (λ = 1.5406 Å for Kα1 and λ = 1.5444 Å for Kα2), operating at 35 kV and 30 mA. The diffraction patterns were obtained between the 2θ range of 5° to 80°, with a step size of 0.02° and a scan speed of 411.2 seconds per step in continuous mode. The goniometer radius measured 240 mm, while the specimen length was kept at 10 mm. A fixed turning slit of 1.0° and a receiving slit of 0.1 mm were employed.

Differential Scanning Calorimetry (DSC)

The thermal characteristics of ITZ, stearic acid, myristic acid, SLN3 and SLN9 were determined using a DSC instrument (DSC TA, Q600, USA). Samples were crimped in a standard aluminum pan and heated from 40 to 400 °C at a heating rate 10 °C/min under constant purging of nitrogen at 20 mL/min.

Stability Study

Physical stability of the optimized ITZ-loaded SLNs was evaluated by assessing both the visual appearance of the nanoparticle formulation for the freshly prepared nanoparticles and those stored at room temperature (25 °C) for one month to detect any changes in physical appearance, such as color change or precipitation. In addition, the size and PDI of the optimized formulations were measured using DLS (Malvern Instruments, UK) for both the fresh and stored formulations to assess any potential changes in size distribution over time.

Drug Release Study

The in vitro drug release from free ITZ solution, and the freeze-dried SLN3 and SLN9 was performed using a dialysis membrane method. An amount of the freeze-dried SLN3 and SLN9 (66.6 mg and 111 mg, respectively) was dispersed in 2 mL of a 1:1 mixture of DMSO and 0.1 M simulated gastric fluid (SGF, pH 1.2) or 0.1 M phosphate-buffered saline (PBS, pH 6.8) containing 1 % v/v Tween 80, which was equivalent to 2 mg/mL of free ITZ solution. The nanoparticles dispersion was then placed in a cellulose dialysis membrane (MWCO 14 kDa, Membra-Cell, USA), which had been pre-soaked overnight in water and washed repeatedly with the release medium before use. The dialysis membrane was firmly tied at both ends using a clamp, and its center part was immersed in 40 mL of the release medium (1:1 DMSO and 0.1 M SGF, pH 1.2 or PBS, pH 6.8, with 1 % Tween 80), kept at 37 ± 1 °C under constant stirring at 100 rpm. At predetermined time intervals, 5 mL of the external dialysis medium was removed and replaced with an equal amount of fresh release medium to keep sink conditions. The concentration of ITZ in the collected samples was measured using UV-visible spectrophotometry at a maximum wavelength (λ_{max}) of 265 nm, based on a calibration curve constructed using a 3:1 ethanol: water mixture over the concentration range of 100 μg/mL to 0.78 μg/mL. An ITZ solution at 2 mg/mL in a liquid mixture of water and DMSO (1:3 v/v) was used as a reference. The experiment was performed in triplicate. The in vitro drug release patterns of solid lipid nanoparticles formulations were compared quantitatively using the similarity factor (f_2). The f_2 value is a logarithmic equivalent square root transformation of the sum of squared differences between two dissolution profiles, as specified by the following equation:

$$f_2 = 50 * \log\left\{\left[1+\frac{1}{n}\sum_{t=1}^{n}\left(R_t - T_t\right)^2\right]^{-0.5} * 100\right\}, \quad (4)$$

where n is the number of sampling time points; R_t is the cumulative percentage of drug released from the reference formulation at time t; and T_t is the cumulative percentage of drug released from the test formulation at the same time point. An f_2 value between 50 and 100 shows similarity between two release patterns, but values below 50 suggest dissimilarity [17].

Statistical Analysis

All tests were performed in triplicate, and the results are reported as mean ± standard deviation, which were calculated using Microsoft Excel software 2021 (version 2503). Statistical analysis was carried out with one-way ANOVA with post hoc Tukey test using IBM SPSS Statistics (version 25). When comparisons involved two independent groups, statistical differences were evaluated using an independent-samples *t*-test. A *p*-value of < 0.05 was considered statistically significant.

Ethical Approval

This study was performed according to the standard procedures and institutional guidelines, and the study protocol was reviewed and approved by the Ethics and Research Registration Committee at the College of Pharmacy, University of Sulaimani (approval number PH143-24, Kurdistan Region, Iraq).

Results and Discussion

Solubility of ITZ in Lipids

Lipid solubility is crucial in the development of lipid-based nanoparticles, especially for hydrophobic drugs like ITZ. Solubility of drug in lipid is one of the most important factors for determining drug loading capacity of the SLNs as well as influencing their release characteristics and bioavailability. Therefore, prior to the formulation of the nanoparticles, the solubility of ITZ in the selected lipids was determined. The results of the solubility studies are shown in Table 2.

Table 2

Solubility of pure ITZ in different solid lipids used to prepare the ITZ loaded SLNs
Data are expressed as mean ±SD, n=3

Lipids	Solubility (mg/g)
Stearic acid	8.72 ± 0.04
Palmitic acid	8.38 ± 0.28
Myristic acid	8.40 ± 0.36

ITZ exhibited comparable solubility in all tested lipids. Stearic acid showed a marginally higher solubilization capacity; however, the differences among the lipids were minimal, indicating a broadly similar affinity of ITZ toward saturated fatty acids with varying carbon chain lengths. Overall, all three lipids appear suitable for ITZ incorporation, with stearic acid offering a slight advantage. Previous research has shown that increased drug solubility in the lipid phase correlates with enhanced encapsulation efficiency and prolonged release capability [18].

Turbidimetric Analysis

The turbidity measurements were used as a rapid and indirect indicator of particle size, aggregation behavior, and dispersion stability of the ITZ-loaded SLNs. Changes in turbidity reflect differences in lipid chain length, surfactant type, and concentration, thereby supporting and complementing the particle size and dispersion stability of the SLNs. Figure 1 showed the results of the turbidity measurements for the prepared ITZ –loaded SLNs. Formulations contained stearic acid with Tween 80 (SLN1, SLN2) exhibited highest turbidity, which can be related to the stiff structure of long-chain lipids (C18) and limited stabilization, resulting in large aggregates [19]. The substitution with Pluronic F127 (in SLN3, SLN4) significantly diminished turbidity, indicating improved steric stability and the production of smaller particles [20]. Palmitic acid formulations exhibited moderate turbidity, with Pluronic F127 (SLN7, SLN8) exceeding Tween 80 (SLN5, SLN6). Myristic acid nanoparticles (SLN9–SLN12) demonstrated the least turbidity due to their shorter chain length (C14) and reduced melting point, which facilitated the formation of smaller, more translucent dispersions, especially in conjunction with Pluronic F127. The increase in surfactant quantity from 1 % to 1.5 % typically reduced turbidity in all formulations [21]. These data collectively indicate that shorter-chain lipids, high sur-

factant concentrations, and the application of Pluronic F127 improve particle dispersion and stability reflected by the reduced turbidity.

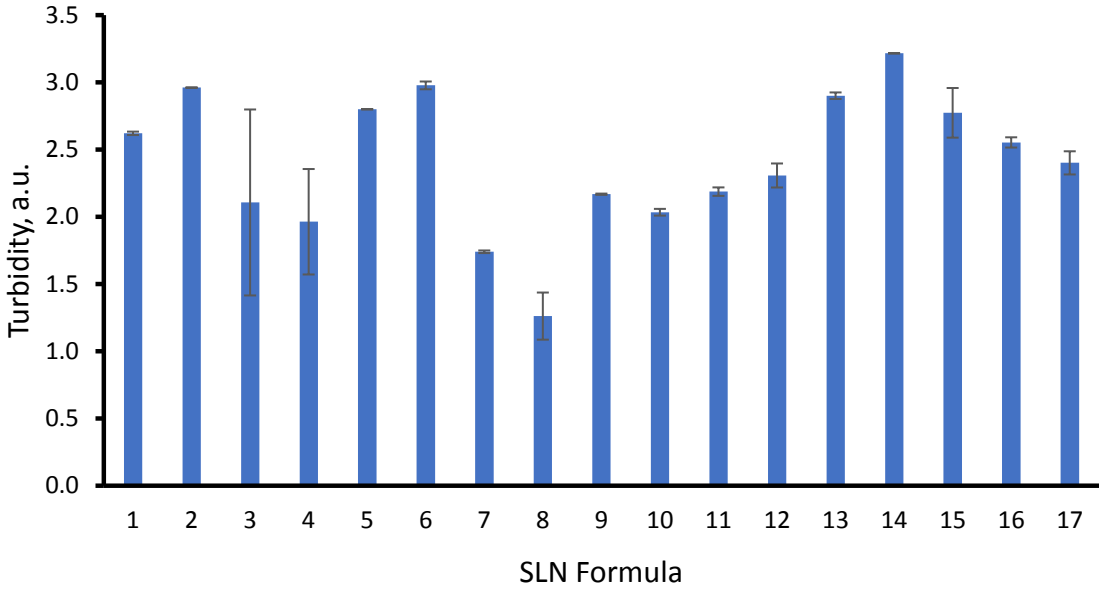

Figure 1. Turbidimetric analysis of ITZ-loaded solid lipid nanoparticle formulations

pH Analysis

Figure 2 showed the pH of the prepared ITZ-loaded SLN formulations. The measured pH values of the formulations varied from 4.7 to 6.1, indicating the impact of lipid and surfactant content. Formulations containing stearic acid (SLN1–SLN4) demonstrated slightly higher pH values. This finding corresponds with the decreased water solubility and increased hydrophobicity of stearic acid, resulting from its long-chain saturated fatty acid structure (C18), which reduces the ionization of its carboxyl groups into the aqueous phase [22]. Conversely, formulation containing myristic acid (C14) SLN9–SLN12 showed the lowest pH values (SLN11 and SLN12, below 4.8), likely due to the increased release of carboxylate ions caused by higher solubility and shorter chain length. Formulations including palmitic acid (C16; SLN5–SLN8) showed intermediate pH values in comparison with stearic and myristic acid-based systems, often varying between 5.2 and 5.8. The pH range indicates a moderate ionization of the carboxyl groups into carboxylate ions in aqueous media, which is associated with the chain length and solubility of palmitic acid in water. Palmitic acid, a medium-chain saturated fatty acid, exhibits lower solubility than myristic acid but higher solubility than stearic acid, resulting in moderate acidity of the dispersion [23].

The type and concentration of surfactants considerably influenced the pH. In all lipid matrices, formulations containing Tween 80 (SLN1, 2, 5, 6, 9, 10) consistently exhibited higher pH values relative to those containing Pluronic F127 (SLN3, 4, 7, 8, 11, 12). Tween 80, a non-ionic surfactant characterized by a polyoxyethylene structure, is recognized for sustaining a relatively neutral pH and facilitating emulsion stabilization without inducing acidification. Conversely, Pluronic F127, a block copolymer of polyethylene and polypropylene oxide, may facilitate the solubilization of lipid components, hereby promoting the ionization of fatty acid carboxyl groups into the aqueous phase and consequently lowering the pH [24]. Additionally, a slight concentration-dependent impact was also observed. In Tween 80 formulations, elevating the content from 1 % to 1.5 % slightly raised the pH, likely due to enhanced micelle formation that sequesters free fatty acids. In contrast, within Pluronic F127 systems, elevated concentrations sometimes resulted in reduced pH values, particularly when combined with myristic acid (SLN 12), which may adversely affect acid-labile drugs [25].

All formulations consistently maintained pH values within the appropriate physiological range for oral administration (pH 4.5–7), indicating their compatibility with the gastrointestinal tract and suggesting a reduced risk of mucosal irritation [22]. Furthermore, formulations with a pH around neutrality are seen as more stable, particularly for pH-sensitive pharmaceuticals such as ITZ, which demonstrates pH-dependent solubility and dissolution [26].

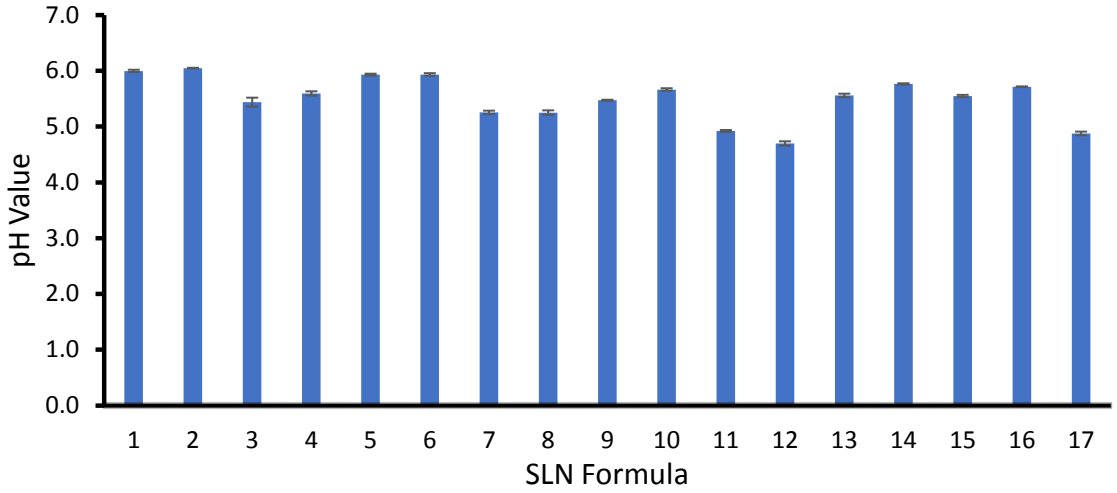

Figure 2. pH of the prepared ITZ-loaded solid lipid nanoparticle formulations

Particle Size, PDI, and Zeta Potential

The particle size and polydispersity of SLNs were significantly affected by the type of lipid, surfactant, and their concentrations. Table 3 shows the Z-average, PDI and zeta potential of the SLN formulations. Formulations based on stearic acid (SLN1–4) produced comparatively smaller particles (550–975 nm) with moderate uniformity, attributed to the rigid crystalline nature of stearic acid, leading to restricted molecular rearrangement during particle formation and thereby limiting particle coalescence and growth. Increased Tween 80 concentration (in SLN2) enhanced size homogeneity, whereas Pluronic F127 (SLN4) produced wider distributions, indicating diminished stabilization with stearic acid [26]. Palmitic acid formulations (SLN5–8) produced larger particles (up to approximately 1975 nm), with Tween 80 resulting in narrower peaks compared to Pluronic F127, especially at a concentration of 1.5 %. Myristic acid-containing SLNs (SLN9–12) exhibited enhanced emulsification with Tween 80 at 1.5 % (SLN10), whereas Pluronic systems maintained greater polydispersity [27]. Figure 3-Panel A shows stearic acid-based SLNs (SLN1–4) exhibited moderately uniform size distributions ranging from 550–975 nm. Figure 3-Panel B shows myristic acid-based SLNs (SLN9–12) displayed slightly broader but well-defined peaks between 600–1500 nm which highlights the influence of lipid type on particle size distribution, allowing direct comparison of lipid-dependent effects. The post-hoc analysis indicated substantial differences in the particle size of different lipid-based SLNs (p = 0.002). Independent samples t-tests indicated a significant effect of surfactant type on the particle size, with Tween 80- and Pluronic F127-stabilized systems having statistically different particle sizes (p = 0.042), indicating changes in interfacial adsorption behavior. SLN13 which contained stearic acid and ethanol remained significantly polydisperse, while SLN14 which contained palmitic acid and ethanol attained monomodal distributions, thereby indicating ethanol's efficacy in improving dispersion. Based on these data, the optimum formulations were determined primarily for having the smallest particle size and the lowest PDI of all formulations, showing excellent nanoscale features and size homogeneity. These formulations were thus regarded the best candidates for further physicochemical and performance evaluation.

Zeta potential analysis demonstrated consistently negative surface charges (−14.4 to −23.5 mV), indicating colloidal stability. Stearic acid-based SLNs demonstrated the greatest negative values, indicating enhanced surface packing and ionization. Tween 80 generally revealed a greater number of charged groups compared to Pluronic F127, hence augmenting surface charge in certain instances (e.g., SLN1 versus SLN3). Increasing surfactant concentration occasionally diminished zeta potential, presumably due to adsorption masking lipid head groups [28]. The addition of ethanol marginally reduced the magnitude of zeta potential, which is ascribed to alterations in interfacial organization. Formulations attaining zeta potentials of approximately −20 mV or lower, specifically stearic acid–Tween 80 and myristic acid–Pluronic F127 systems, exhibited advantageous electrostatic stabilization. Overall, although the absolute zeta potential values were moderate, the presence of non-ionic surfactants indicated that steric stabilization, in addition to electrostatic repulsion, helped to preserve colloidal stability. Surface-adsorbed surfactant chains create a hydrated barrier that reduces particle–particle interactions and helps stabilize nanoparticles, even when zeta potentials are

below ±30 mV. As a result, the observed stability of selected formulations is most likely due to a mixed electrostatic-steric stabilization mechanism, similar to that described for SLNs stabilized with Tween 80 or Pluronic surfactants [29].

Table 3

Physicochemical properties of the prepared ITZ loaded SLNs. Data are expressed as mean ±SD, *n* = 3

Formulation	Size (Z-average), nm	PDI	Zeta potential, mV
SLN1	591 ± 40	0.680 ± 0.120	–23.53 ± 0.85
SLN2	676 ± 7	0.497 ± 0.039	–16.83 ± 0.37
SLN3	550 ± 30	0.615 ± 0.075	–14.56 ± 0.41
SLN4	975 ± 52	0.759 ± 0.036	–21.40 ± 0.70
SLN5	1763 ± 350	0.922 ± 0.134	–20.46 ± 0.80
SLN6	1975 ± 66	0.606 ± 0.030	–16.96 ± 0.68
SLN7	1054 ± 33	0.522 ± 0.037	–15.36 ± 0.56
SLN8	955 ± 13	0.558 ± 0.075	–17.26 ± 0.37
SLN9	664 ± 78	0.634 ± 0.069	–20.20 ± 0.36
SLN10	1562 ± 161	0.705 ± 0.021	–19.76 ± 0.49
SLN11	1546 ± 71	0.705 ± 0.021	–21.76 ± 0.15
SLN12	1403 ± 35	0.490 ± 0.051	–21.46 ± 0.55
SLN13	939 ± 34	0.575 ± 0.030	–16.10 ± 0.26
SLN14	4008 ± 517	0.755 ± 0.147	–14.40 ± 0.43
SLN15	1748 ± 185	1 ± 0.000	–18.13 ± 0.41
SLN16	2745 ± 131	1 ± 0.000	–17.26 ± 0.57
SLN17	968 ± 42	0.371 ± 0.036	–17.50 ± 0.55

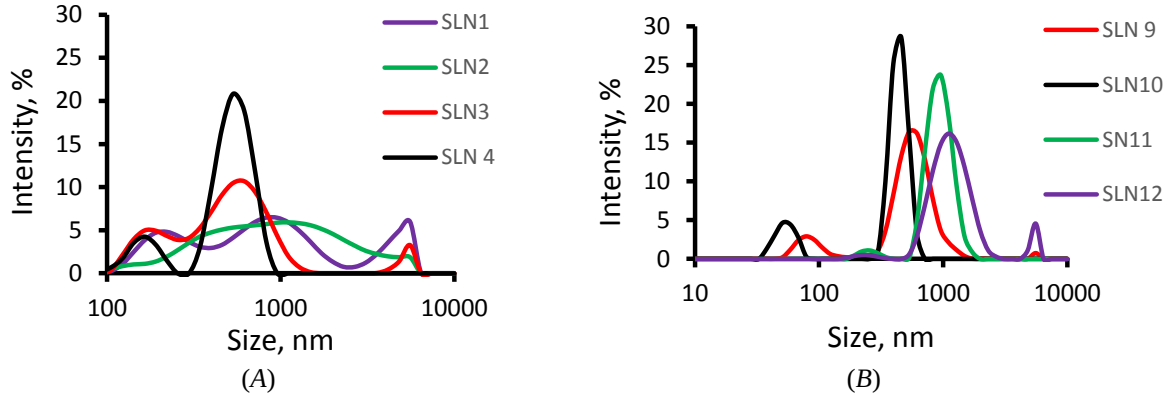

Figure 3. Dynamic light scattering size distribution curves of the ITZ loaded SLNs.
(*A*) SLN 1, 2, 3 and 4 were formulated with stearic acid as the lipid carrier;
(*B*) SLN 9, 10, 11, and 12 were formulated with myristic acid as the lipid carrier

Among the prepared ITZ-loaded SLN formulations, SLN3 and SLN9 were selected as the optimum formulations based on their smaller particle size as determined by DLS and the lowest PDI indicating uniform and stable nanoparticles. Notably, SLN9 incorporated myristic acid, an unexplored lipid for ITZ SLNs, highlighting its potential as a novel lipid matrix for enhancing formulation performance, warranting further in-depth evaluation as a promising oral delivery system for ITZ.

Effects of SLNs on ITZ Solubility

ITZ exhibits poor aqueous solubility, which is further influenced by its pH-dependent ionization behavior. As show in Figure 4, the shake-flask solubility study demonstrated extremely low solubility for pure ITZ at both pH 1.2 and pH 6.8, with concentrations remaining in the range of 67.067 µg/mL at pH 1.2 and 0.306 µg/mL at pH 6.8. The solubility was slightly higher under acidic conditions, consistent with ITZ being a weakly basic drug (pKa ≈ 3.7), which favors protonation and partial dissolution in gastric-like environments [30]. However, even at pH 1.2, the solubility of pure ITZ was negligible compared to its therapeutic

requirements, confirming the need for solubility-enhancing formulations. Encapsulation of ITZ into SLNs markedly enhanced its solubility at both tested pH conditions. At pH 1.2, SLN3 achieved solubility values close to 2900 µg/mL, while SLN9 reached 3369 µg/mL. At pH 6.8, the solubility improvement was even more remarkable compared to the pure drug. SLN3 achieved 10.59 µg/mL, and SLN9 showed the highest solubility 26.94 µg/mL. These enhancements reflect a multifactorial effect of lipid type and surfactant characteristics. The superior performance of SLN9 over SLN3 may be attributed to the formulation differences which are the lipid chain length; Myristic acid (C14) in SLN9 possesses a shorter hydrocarbon chain than stearic acid (C18) used in SLN3. Shorter-chain fatty acids generally form less-ordered crystalline lattices with lower melting points, enhancing solubilization of lipophilic drugs within the lipid matrix [31]. Tween 80 in SLN9 is a nonionic surfactant with a high hydrophilic-lipophilic balance (HLB ≈ 15), facilitating stronger interfacial stabilization and promotes solubilization of poorly water-soluble drugs. In contrast, Pluronic F127, a block copolymer, often stabilizes particles through steric mechanisms but may provide lower solubilization capacity in the aqueous phase [11]. These differences likely explain the higher solubility observed for SLN9 at both acidic and near-physiological pH.

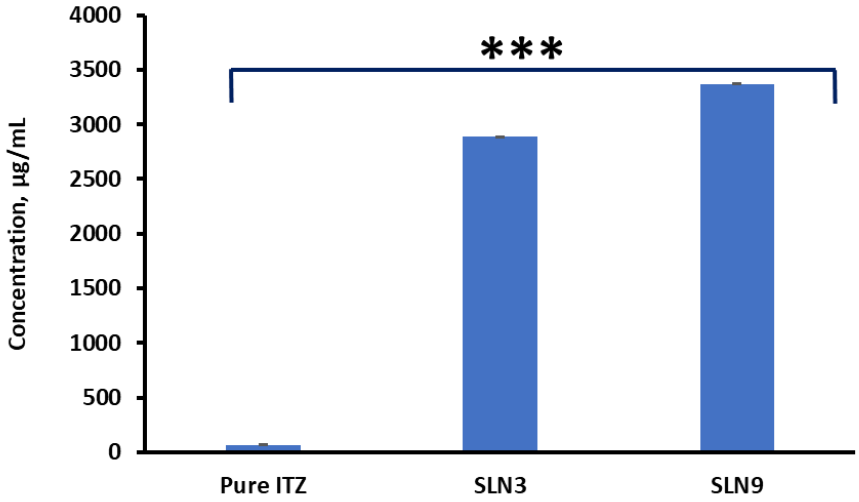

(*A*)

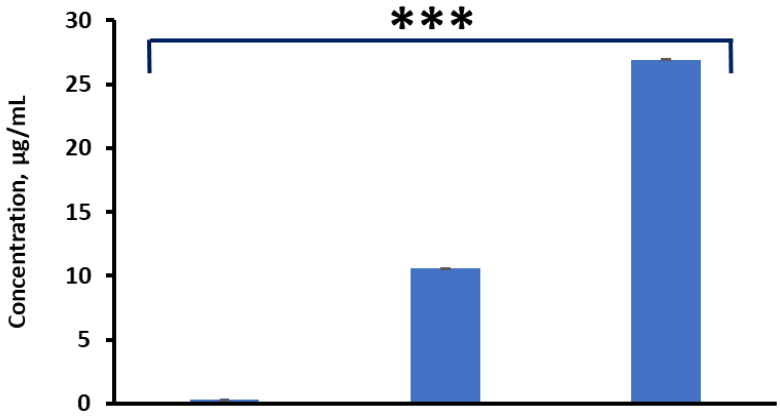

(*B*)

Figure 4. Saturation solubility of ITZ in its pure form as well as in SLN formulations (SLN3 and SLN9) (*A*) in simulated gastric fluid (pH 1.2) and (*B*) in phosphate-buffered saline (pH 6.8).
*** indicates statistically significant difference in solubility ($p < 0.001$). Statistically significant differences were observed between pure ITZ and SLN3, pure ITZ and SLN9, as well as between SLN3 and SLN9

Determination of Yield, Encapsulation Efficiency (EE), and Loading Capacity (LC)

The lyophilized SLNs appeared as a fine, white powder with a slightly fluffy texture, with no visible signs of aggregation or caking immediately after freeze-drying, suggesting good preservation of particle integrity. Upon reconstitution in simulated gastric fluid (pH 1.2) and phosphate-buffered saline (pH 6.8), the powders readily dispersed, yielding suspensions with a uniform and colloidally stable appearance. The yield of the freeze-dried SLNs was modest, with SLN9 (57.9 ± 6.6 %) indicating some higher recovery than SLN3 (50.03 ± 3.55 %), likely attributable to variations in lipid and surfactant composition influencing particle aggregation and collection. SLN3 had a markedly higher encapsulation efficiency (97.04 ± 0.004 %) compared to SLN9 (42.69 ± 0.02 %), indicating enhanced drug encapsulating capability. This can be due to the superior compatibility of ITZ with stearic acid and the denser lipid matrix in SLN3. Additionally, SLN3 exhibited superior drug loading (3 ± 0.1 %) compared to SLN9 (1.8 ± 0.17 %), underscoring its potential as a more effective drug delivery system for poorly water-soluble drugs. These findings correlate with prior studies indicating that lipid type and surfactant concentration significantly affect EE and LC [32].

FTIR Spectroscopy

FTIR spectroscopy was utilized to examine possible interactions between ITZ and solid lipids (stearic acid, myristic acid) in SLN3 and SLN9 formulations. As shown in Figure 5, pure ITZ displayed distinct peaks at 3120 cm^{-1} (aromatic C–H stretching), 2970 cm^{-1} (aliphatic C–H stretching), 1700 cm^{-1} (C=O stretching), 1600 cm^{-1} and 1500 cm^{-1} (aromatic C=C stretching), along with a pronounced band near 1045 cm^{-1} attributed to C–O stretching. The observed bands correlate with previously documented FTIR spectra of ITZ, signifying its stable chemical structure [33].

Stearic acid (SA) and myristic acid (MA) exhibited significant peaks at 2850–2920 cm^{-1}, indicative of symmetric and asymmetric C–H stretching vibrations, along with a distinct peak at approximately 1700 cm^{-1}, corresponding to the C=O stretching of carboxylic acid. These characteristics are indicative of long-chain saturated fatty acids, consistent with prior research [34]. The SLN3 formulation, comprising stearic acid and Pluronic F127, preserved the significant C–H stretching peaks at 2850 and 2920 cm^{-1}, accompanied by a considerable expansion of the O–H stretching area (~3000–3500 cm^{-1}), suggesting potential hydrogen bonding. The C=O peak exhibited a modest shift and diminished intensity, indicating interaction between ITZ and the lipid matrix [34]. Likewise, SLN9 (composed of myristic acid and Tween 80) exhibited retained C–H and C=O peaks of the lipid; however, the ITZ peaks at 1600–1500 cm^{-1} and 1045 cm^{-1} were slightly reduced. This indicates that ITZ was molecularly diffused within the lipid matrix, resulting in an altered crystalline structure, as evidenced by the reduced intensity of typical ITZ peaks [35].

The lack of significant ITZ-specific peaks in the SLN spectra, along with the observation of shifted or widened bands, suggests possible encapsulation and molecular interaction between the drug and lipids. The alteration or absence of specific ITZ peaks during the formulation of SLNs has been documented by others as a sign of effective drug entrapment and conversion from crystalline to amorphous state [36].

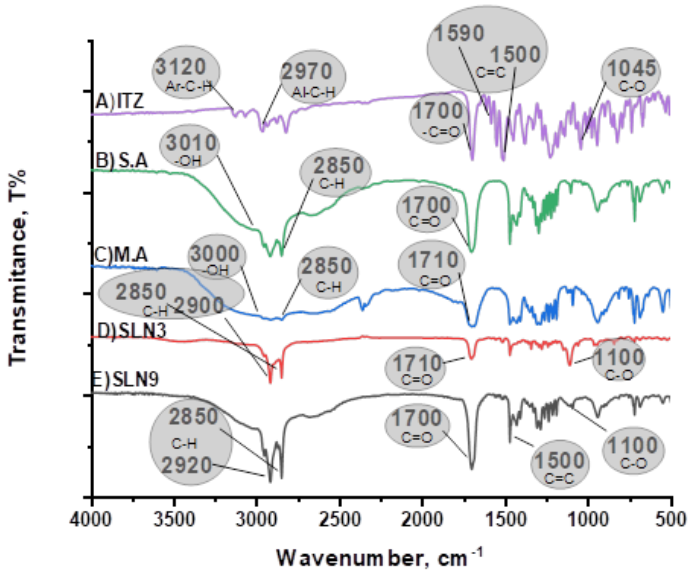

Figure 5. FTIR spectra for ITZ, stearic acid (S.A), myristic acid (M.A), SLN3 and SLN9

Transmission Electron Microscopy (TEM)

Transmission Electron Microscopy (TEM) was utilized to investigate the internal structure and morphology of the optimized SLN3 and SLN9 formulations. The TEM micrographs of ITZ-loaded SLNs (SLN3 and SLN9) (Figure 6) reveal discrete nanoparticles with a predominantly spherical to quasi-spherical morphology. Individual SLNs appear as relatively light, rounded features, consistent with the expected morphology of lipid-based nanoparticles. The darker contrast regions observed in the images do not represent the morphology of single nanoparticles; instead, they arise from overlapping particles and localized thickening of the lipid matrix during sample deposition and drying on the TEM grid. Such contrast variations are inherent to TEM imaging of soft lipid nanocarriers and reflect differences in electron density rather than particle irregularity [37].

The mean particle size detected using TEM (Figure 7 and 8) were 102 nm and 244 nm for SLN3 and SLN9, respectively and was slightly smaller than those derived from DLS measurements. The discrepancy between particle sizes determined by DLS and TEM should be interpreted in light of the fundamentally different physical principles governing these techniques [38]. DLS provides an ensemble-averaged, intensity-weighted hydrodynamic diameter, which is highly sensitive to polydispersity, minor populations of larger particles, transient aggregation, concentration-dependent diffusion, and electrostatic double-layer effects. In contrast, TEM yields number-based, projection-dependent particle dimensions obtained under dry-state and high-vacuum conditions, which may underestimate soft, hydrated or low-density surface structures [39]. Furthermore, particle shape anisotropy, contrast limitations, and sample-preparation artefacts can further amplify apparent size mismatches. As emphasized by Filippov et al. [39], substantial DLS–TEM size discrepancies arise primarily from methodological bias rather than experimental inconsistency, and therefore the observed size difference in the present study is consistent with the expected ensemble-scattering nature of DLS compared with the single-particle visualization of TEM.

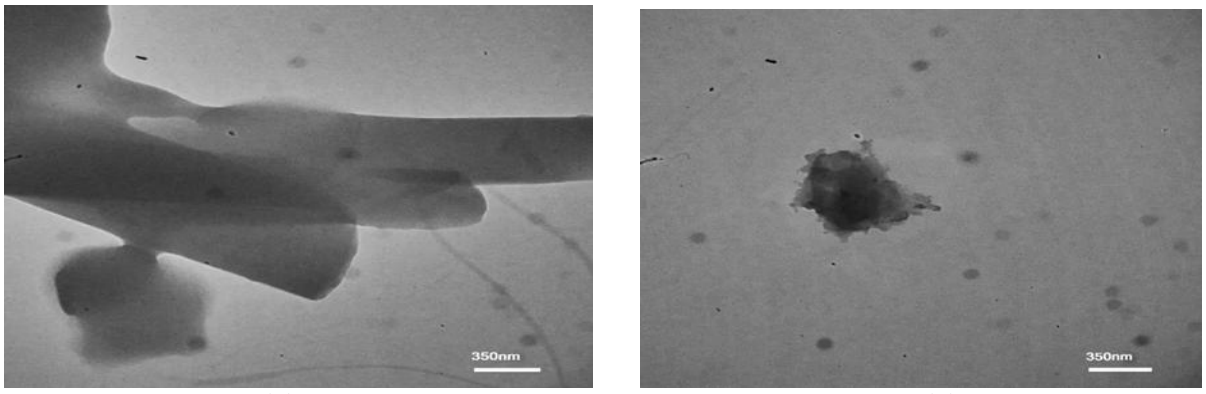

(*A*) (*B*)

Figure 6. Transmission electron microscopy (TEM) images of ITZ loaded SLNs, (*A*) SLN3 and (*B*) SLN9

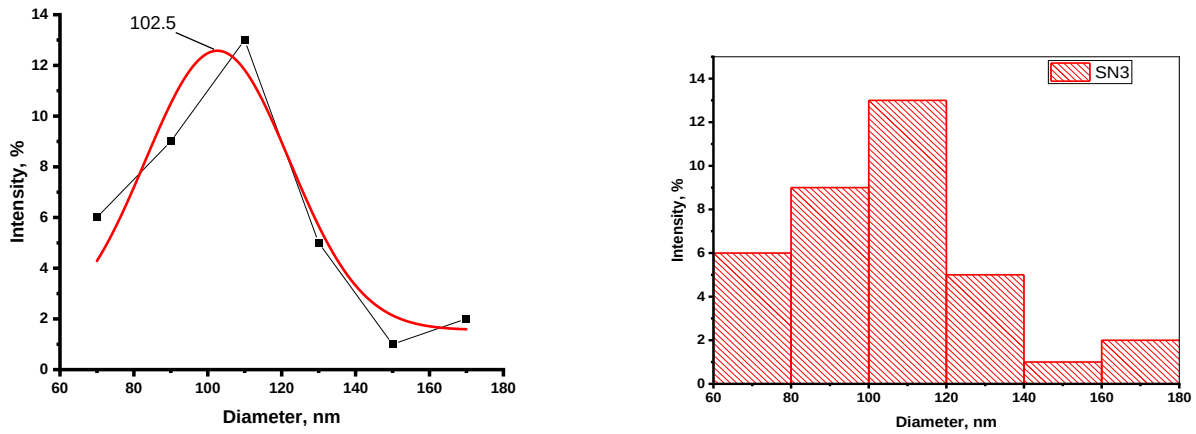

(*A*) (*B*)

Figure 7. Transmission electron microscopy (TEM) derived size distribution curve (*A*) and histogram (*B*) of SLN3 based on TEM analysis

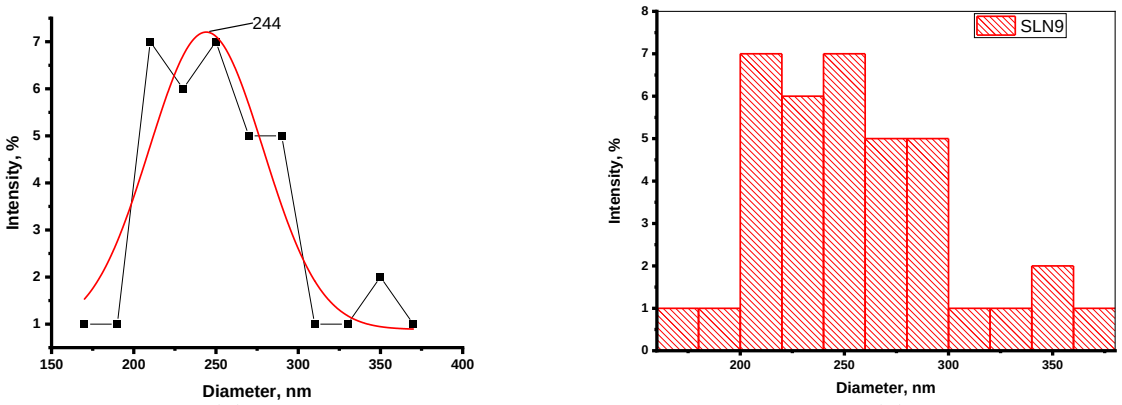

(*A*) (*B*)

Figure 8. Transmission electron microscopy (TEM) derived size distribution curve (*A*) and histogram (*B*) of SLN9 based on TEM analysis

Field Emission Scanning Electron Microscopy (FESEM)

Field Emission Scanning Electron Microscopy (FESEM) was employed to examine the morphological characteristics and surface properties of SLN3 and SLN9. Figure 9 illustrates that SLN3, synthesized using stearic acid and Pluronic F127, had primarily spherical particles with a relatively uniform distribution. The image displayed a certain level of surface roughness, likely due to the utilization of stearic acid as the principal lipid matrix. Conversely, the FESEM images of SLN9, composed of myristic acid and Tween 80, exhibited more distinct and well-separated spherical particles with smoother surfaces. This may be due to the shorter carbon chain length of myristic acid, leading to reduced cohesive interactions within the lipid matrix, resulting in more uniformly distributed particles. Prior research has indicated that the lipid type significantly influences the particle morphology of SLNs [40]. The differences in SLN morphology observed between TEM and FESEM images are mainly attributed to differences in sample preparation and imaging mechanisms. TEM requires drying and high-vacuum conditions, which may induce particle deformation, aggregation, or partial collapse of the solid lipid matrix, leading to irregular morphologies [38]. In contrast, FESEM primarily provides surface-topographical information and generally preserves external morphology more effectively, although some aggregation may still occur during solvent evaporation and conductive coating. Together, the TEM and FESEM data provide complementary information, supporting the successful formation of nanosized, predominantly spherical lipid nanoparticles [41]. From the FESEM study, it was revealed that the size of optimal ITZ-loaded SLNs was 69 ± 22 nm and 45 ± 19 nm for SLN3 and SLN9, respectively. The FESEM-derived particle size distribution curve and histogram are illustrated in Figure 10 and 11.

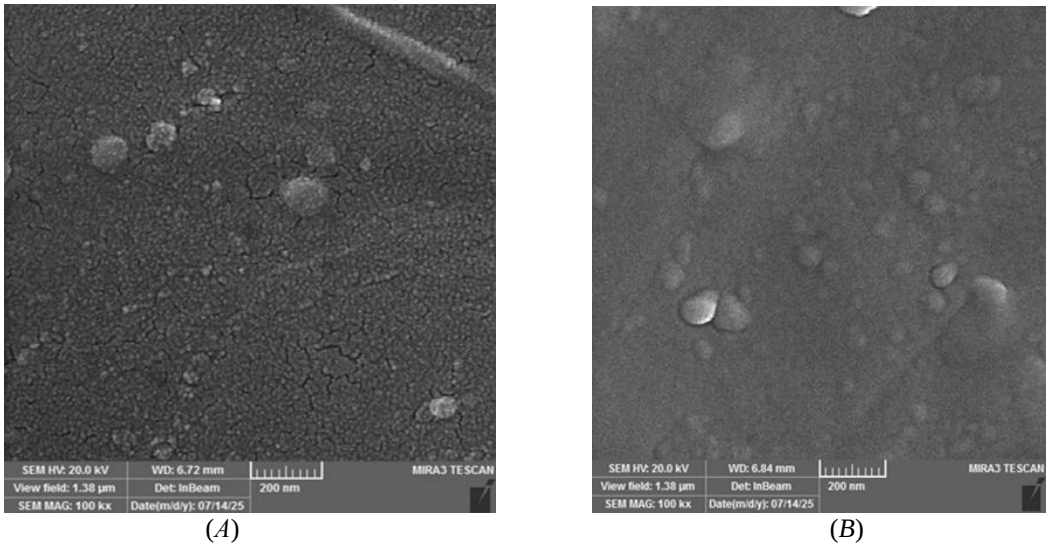

(*A*) (*B*)

Figure 9. Field Emission Scanning Electron Microscopy (FESEM) images of the optimal ITZ-loaded SLNs (*A*) SLN3 and (*B*) SLN9

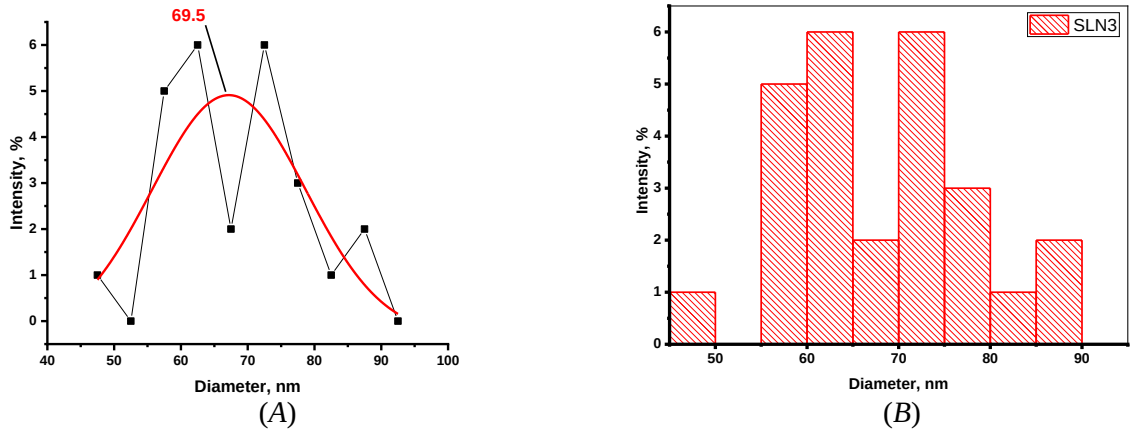

(*A*) (*B*)

Figure 10. FESEM-derived particle size distribution curve (*A*) and histogram (*B*) of SLN3

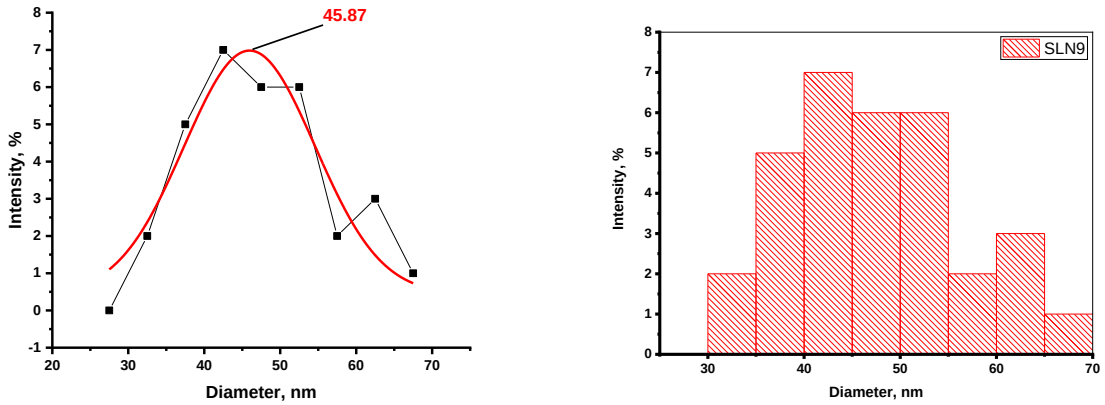

(*A*) (*B*)

Figure 11. FESEM-derived particle size distribution curve (*A*) and histogram (*B*) of SLN9

Powder X-Ray Diffraction (PXRD)

Powder X-ray diffraction (XRD) was performed to evaluate the crystalline properties of pure ITZ, stearic acid (SA), myristic acid (MA), and their respective solid lipid nanoparticle formulations (SLN3 and SLN9). Figure 12 shows that pure ITZ exhibited characteristic sharp and intense peaks within the 2θ range of 10° to 30°, a pattern indicative of its extremely crystalline characteristics. These results correspond with previously documented diffractograms of pure ITZ, which often display characteristic polymorphism attributes [42].

Stearic acid and myristic acid exhibited distinct diffraction peaks around 2θ = 21°–24°, stearic acid showing reflections at about 21.66° and 24.26°. Likewise, myristic acid was shown to display strong broad-but-sharp peaks around 20.51°, 21.85°, and 24.34° [43]. Conversely, the XRD patterns of SLN3 and SLN9 demonstrated a significant decrease in peak intensity and sharpness, with broad bands substituting the distinct sharp peaks which could indicate a change from a crystalline to an amorphous state, signifying the effective encapsulation of ITZ within the lipid matrix [11]. The absence or considerable attenuation of distinctive peaks in both ITZ and the lipids indicates a loss of long-range molecular order, possibly resulting from high-energy emulsification processes followed by rapid cooling during SLN synthesis. This transition is advantageous for poorly soluble drugs such as ITZ, as the amorphous state typically correlates with increased dissolution rates and greater bioavailability [44]. PXRD results demonstrated that the crystalline peaks of ITZ and lipids were significantly broadened or attenuated in SLN3 and SLN9, indicating the molecular embedding of ITZ within a solid lipid matrix. Importantly, the presence of broad lipid diffraction peaks confirms that the lipid phase remained solid, which differentiates these formulations from liquid lipid-based systems such as nanoemulsions or microemulsions, which lack solid-state diffraction patterns. The notable change in the diffraction patterns of SLN3 and SLN9, in contrast to the pure drug and lipid components, clearly indicates effective molecular embedding and diminished crystallinity, which is a favorable result in nanocarrier-based drug delivery.

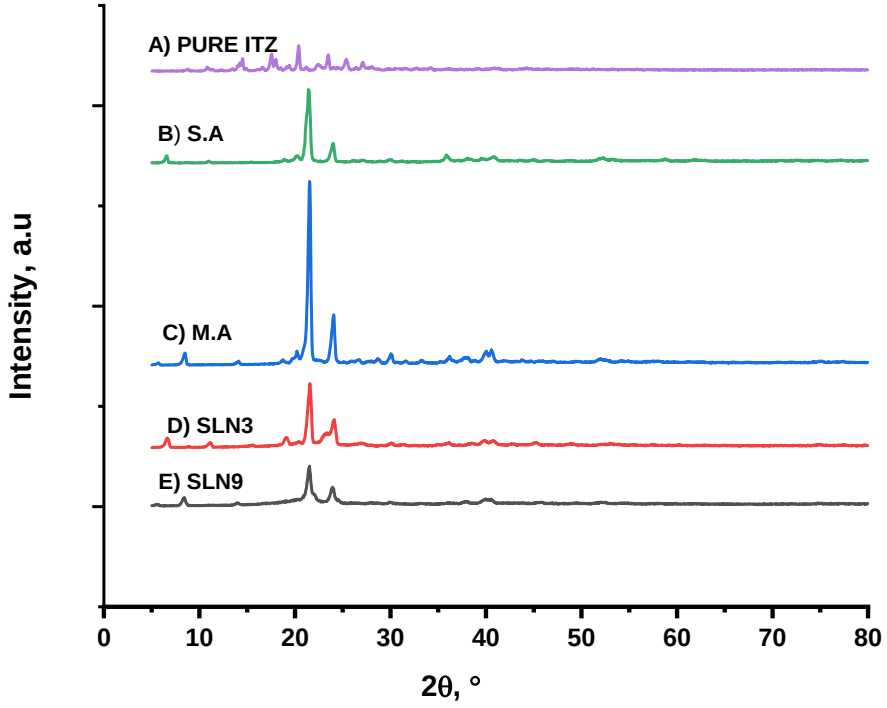

Figure 12. Powder X-ray diffractograms of Pure ITZ, stearic acid (S.A), myristic acid (M.A), SLN3 and SLN9

Differential scanning calorimetry (DSC)

The DSC analysis showed that pure ITZ exhibited a sharp endothermic peak at approximately 167 °C, corresponding to its melting point and confirming its crystalline nature [45]. Figure 13 shows that stearic acid (SA) and myristic acid (MA) exhibited distinct endothermic peaks at roughly 69 °C and 54 °C, respectively, indicative of their melting temperatures. These results correspond with literature values for the melting transitions of SA and MA, signifying their pure and crystalline forms [46].

The SLN formulations (SLN3 and SLN9) demonstrated unique thermal characteristics in contrast to their pure constituents. SLN3, consisting of stearic acid and Pluronic F127, exhibited a broad and diminished endothermic peak at approximately 60–65 °C, whilst SLN9, comprising of myristic acid and Tween 80, demonstrated a similarly broadened peak around 52 °C. The distinctive melting peak of ITZ was either absent or markedly diminished in the thermograms of both SLN3 and SLN9. The absence or alteration of the drug's melting peak in the SLNs indicates that ITZ was either molecularly dispersed within the lipid matrix or present in an amorphous state, rather than in a crystalline form. Such modifications are frequently reported in lipid-based nanoparticle systems and signify effective drug encapsulation and amorphization, potentially improving dissolution rates and bioavailability [47].

The observed decrease in peak intensity and enthalpy values in the lipid matrix of the SLNs may be due to the disruption of the lipid crystal structure caused by the inclusion of drugs and surfactants. The interplay between lipid chains and surfactants like Tween 80 or Pluronic F127 can create defects in the lipid matrix, diminishing crystallinity and enhancing drug loading capacity [48]. DSC analysis further supported the solid nature of the lipid nanoparticles, showing defined melting transitions of the lipids in SLN3 and SLN9, while the characteristic melting peak of ITZ was absent or markedly diminished. These results are consistent with the amorphization and molecular incorporation of ITZ into a solid lipid core, confirming the formation of SLNs rather than liquid lipid-based systems. The DSC data robustly indicates a successful integration of ITZ into the SLN systems and demonstrates a decrease in drug crystallinity, a favorable attribute for improving solubility and release profiles of poorly soluble drugs.

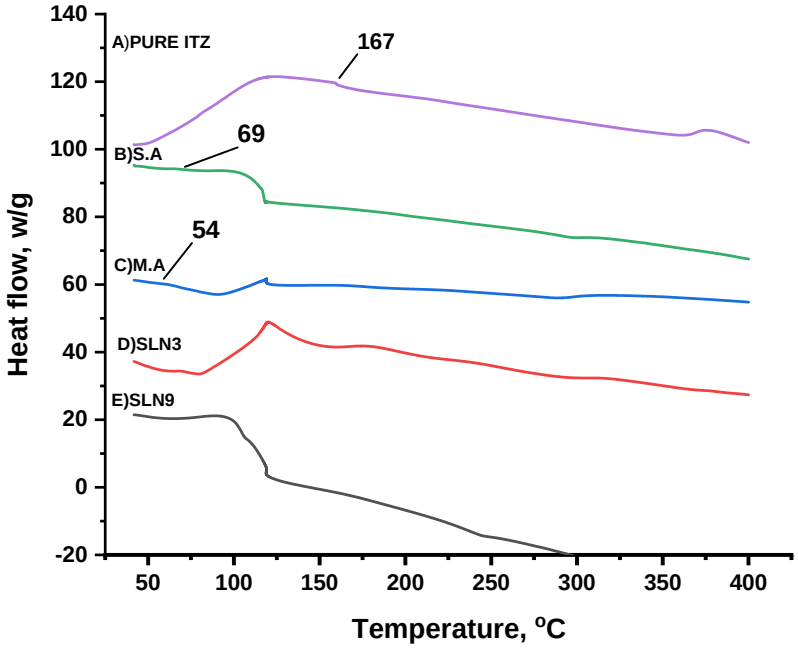

Figure 13. DSC thermograms of Pure ITZ, stearic acid (S.A), myristic acid (M.A), SLN3 and SLN9

Stability Study

The physical stability study revealed marked differences in particle size and PDI between the two formulations, SLN3 and SLN9. SLN3, composed of stearic acid and Pluronic F127, demonstrated a particle size of 550 ± 30 nm and a PDI of 0.61 ± 0.0367 immediately post-preparation (Table S3). After one month, the particle size exhibited a marginal rise to 583 ± 41 nm, while the PDI significantly decreased to 0.533 ± 0.082, while after six months the particle size exhibited a marginal rise to 835 ± 27 nm, PDI decreased to 0.519 ± 0.081 indicating a relatively steady particle dispersion [49]. Conversely, SLN9, comprising myristic acid and Tween 80, exhibited a gradual increase in particle size from 664 ± 78 nm to 2856 ± 102 nm during the six month-storage, accompanied by an elevation in PDI from 0.634 ± 0.069 to 1, signifying some aggregations and a decline in physical stability. The instability may be ascribed to the shorter carbon chain of myristic acid, which likely results in diminished van der Waals interactions and reduced structural rigidity relative to longer-chain fatty acids such as stearic acid [50]. The slight fluctuations in SLN3's particle size and PDI values indicate that it preserved colloidal stability during the specified storage conditions. The observed changes in SLN9 highlight the importance of lipid selection and surfactant type in formulating stable SLNs, suggesting that shorter-chain lipids or particular surfactant type can lead to moderate alterations in particle size and dispersion without necessarily compromising functional performance [51].

Drug Release Study

The *in vitro* release study conducted at pH 1.2, demonstrated notable variations in the release profiles of pure ITZ, SLN3 and SLN9 (Figure 14, A). DMSO was added to the release medium due to its strong solubilizing ability for the highly hydrophobic drug ITZ, ensuring complete dispersion and accurate quantification. Tween 80, a non-ionic surfactant, was included in the release medium to enhance ITZ solubility and maintain sink conditions. Although these conditions do not fully replicate the gastrointestinal environment, they are commonly employed in *in vitro* release studies of poorly soluble drugs to provide reproducible and reliable measurements of formulation performance [52]. Pure ITZ exhibited a gradual and limited release, achieving roughly 25 % after 2880 minutes. This corresponds with the established low aqueous solubility and pH-dependent dissociation characteristics of ITZ, which has a pKa of around 3.7, demonstrating diminished solubility at neutral pH but enhanced solubility in extremely acidic environments [31]. Nonetheless, even in acidic environments, its crystalline structure and lipophilicity result in dissolution-limited release, explaining the level that was seen following the initial stages [53]. Conversely, SLN3, formulated with stearic acid and Pluronic F127, exhibited a markedly superior release profile, attaining nearly 55 % within the same timeframe. The improved and sustained release can be attributable to important formulation features; Pluronic F127 enhances wetting and drug stability in the medium, whereas stearic acid produces a stiff lipid

matrix that regulates release via erosion and diffusion [27]. Notably, SLN9 containing myristic acid and Tween 80 demonstrated a moderate release of around 22 % at 1440 minutes, which decreased marginally by 2880 minutes. The enhanced efficacy of SLN3 relative to SLN9 highlights the essential influence of lipid composition and surfactant choice. Pluronic F127, a block copolymer with a hydrophilic-lipophilic balance, may provide superior drug retention and extended release compared to Tween 80 in acidic environments [27]. The data robustly indicate that SLNs, particularly those composed of stearic acid and Pluronic F127, effectively enhance the release of poorly soluble drug such as ITZ under gastric conditions, potentially leading to increased oral bioavailability.

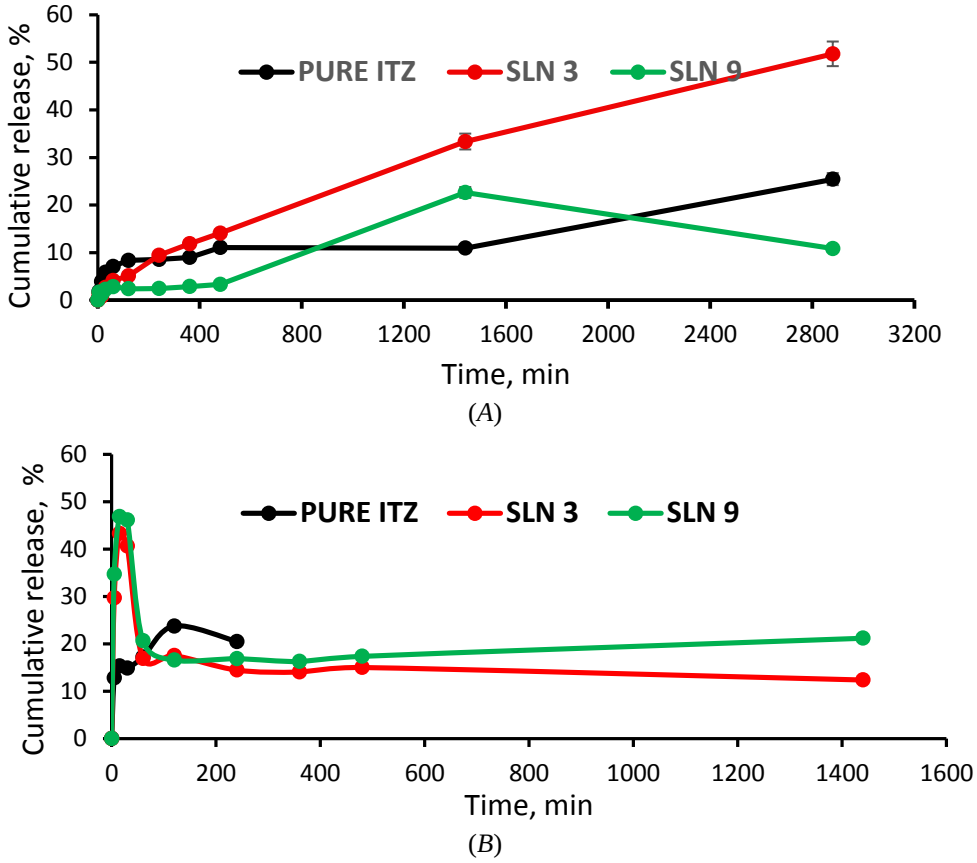

Figure 14. *In vitro* drug release profiles of pure ITZ, SLN 3 and SLN 9 (*A*) in simulated gastric fluid (pH 1.2), and (*B*) in phosphate buffered saline (pH 6.8), $n = 3 \pm SD$

The *in vitro* release profile of pure ITZ, SLN3 and SLN9 at pH 6.8 (Figure 14, B), demonstrated significantly distinct behaviors relative to acidic circumstances. All formulations exhibited an initial burst release during the first 30 minutes, subsequently transitioning to either an equilibrium or a gradual progressive release over 24 hours. Pure ITZ exhibited an initial release of roughly 25 %, subsequently stabilizing with negligible further increase. This trend underscores the notably inadequate aqueous solubility of ITZ at neutral to alkaline pH, which can be due to its weakly basic properties (pKa ~3.7). At pH levels exceeding 6, the drug remains unionized and demonstrates diminished solubility, hence restricting its dissolution in the intestinal milieu [54]. SLN3 demonstrated an initial rapid release within the first few minutes, succeeded by a gradual decrease, indicating potential recrystallization or drug re-adsorption onto the lipid surface, a phenomenon sometimes noted in lipid-based systems due to precipitation from supersaturation. The inadequate solubility of stearic acid-based carriers in intestinal fluid, coupled with the reduced solubility of ITZ at this pH, may lead to drug entrapment within the matrix and restricted diffusion [55]. Conversely, SLN9 had the largest cumulative release at pH 6.8, with sustained release exceeding 20 % by 1500 minutes. This effect may be ascribed to the shorter fatty acid chain of myristic acid [56]. The decrease in release at pH 6.8 can be attributed to ITZ's poor solubility under near-neutral conditions, leading to precipitation. SLN3 shows a more pronounced decline due to the rigid stearic acid matrix, whereas SLN9 maintains higher release owing to

greater matrix fluidity from myristic acid [57]. Overall, the pH-responsive release reflects both ITZ solubility and lipid matrix properties, including crystallinity, chain length, and fluidity. Thus, the differences between SLN3 and SLN9 arise from combined drug–matrix interactions rather than solubility alone. The disparity in performance between SLNs and pure ITZ emphasizes the significance of lipid-surfactant synergy and pH responsiveness. Although SLNs are typically formulated to improve solubility and extend release, their efficacy at intestinal pH is significantly dependent on matrix fluidity, drug-lipid compatibility, and surfactant activity. The data indicate that SLN9 may provide a superior release profile under intestinal conditions compared to SLN3, rendering it a more suitable option for releasing the drug at intestinal pH (around 6–7.4) which could allow drug targeting to the intestine. To assess the *in vitro* release behavior of lipid-based formulations, a similarity factor (f_2) study was done between SLN3 and SLN9. At pH 1.2, the computed f_2 value was less than 50, indicating different release profiles due to lipid chain length and surfactant type. SLN3, containing stearic acid-Pluronic F127, provided more prolonged release under acidic conditions than SLN9, containing myristic acid-Tween 80. At pH 6.8, the f_2 value remained under 50, indicating formulation-dependent and pH-responsive release behavior. The relatively larger release of SLN9 at intestinal pH may be due to increased matrix fluidity caused by myristic acid's shorter fatty acid chain [58].

Conclusions

The successful development of ITZ-loaded SLNs illustrates their promise as a novel drug delivery technology for improving the solubility and bioavailability of ITZ. This study showed that the selection of lipids and surfactants markedly affects the physicochemical characteristics of SLNs, such as particle size, stability, and encapsulation efficiency. The results indicated that formulations including stearic acid and Pluronic F127 produced smaller particle sizes and enhanced stability over time, demonstrating their appropriateness for oral delivery. The solubility experiments indicated a significant enhancement in ITZ solubility when encapsulated in SLNs, with solubility efficiencies markedly above those of pure ITZ. This improvement is due to the nanoscale dimensions of the particles, which increase the surface area for dissolving, and the establishment of a molecularly dispersed state within the lipid matrix that inhibits recrystallization. Furthermore, the physical stability of the formulations over time demonstrates their suitability for pharmaceutical applications, with SLN3 showing negligible alterations in particle size and dispersion after one month of storage. The research indicates that SLNs markedly improve the release of poorly soluble ITZ in different pH levels. SLN3, comprising stearic acid and Pluronic F127, demonstrates superior performance in acidic environments, whereas SLN 9, which includes myristic acid and Tween 80, exhibits enhanced release in intestinal circumstances. In conclusion, the study confirms the usefulness of SLNs in enhancing the solubility, controlling drug release and stability of ITZ while also opening the way for additional research into the *in vivo* performance and therapeutic effectiveness of these formulations. Future studies should concentrate on refining SLN formulations for targeted therapeutic uses and performing pharmacokinetic assessments to evaluate their efficacy in clinical environments.

Supporting Information

The Supporting Information is available free at https://ejc.buketov.edu.kz/ejc/article/view/652/359

*Author Information**

**The authors' names are presented in the following order: First Name, Middle Name and Last Name*

Darya Wahhab Kareem — MSc Student, Department of Pharmaceutics, College of Pharmacy, University of Sulaimani, Sulaymaniyah, Zanko Street, 46001, Kurdistan Region, Iraq; e-mail: darya.kareem@univsul.edu.iq

Twana Mohammed M. Ways (*corresponding author*) — Assistant Professor, Department of Pharmaceutics, College of Pharmacy, University of Sulaimani, Sulaymaniyah, Zanko Street, 46001, Kurdistan Region, Iraq; e-mail: twana.mohammed@univsul.edu.iq; https://orcid.org/0000-0002-7595-2159

Author Contributions

The manuscript was written through contributions of all authors. All authors have given approval to the final version of the manuscript. CRediT: ***Darya Wahhab Kareem*** conceptualization, data curation, investigation, methodology, validation, visualization, formal analysis, writing-original draft, writing-review & edit-

ing; **Twana Mohammed M. Ways** conceptualization, data curation, investigation, formal analysis, resources, supervision, validation, writing-original draft, writing-review & editing.

Acknowledgments

The authors gratefully acknowledge the University of Sulaimani for its support and for providing the facilities necessary to carry out this study.

Conflicts of Interest

The authors declare no conflict of interest.

References

1 Alam, S., Iqbal, Z., Ali, A., Khar, R. K., Ahmad, F. J., Akhter, S., & Talegaonkar, S. (2009). Microemulsion as a Potential Transdermal Carrier for Poorly Water Soluble Antifungal Drug Itraconazole. *Journal of Dispersion Science and Technology*, *31*(1), 84–94. https://doi.org/10.1080/01932690903107265

2 Chhatbar, M., Borkhataria, C., Patel, O., Raichura, K., Pethani, T., Parmar, G., Mori, D., & Manek, R. (2025). Enhancing the solubility and bioavailability of itraconazole through pharmaceutical cocrystallization: A promising strategy for drug formulation. *Journal of Pharmaceutical Sciences*, *114*(6), 103770. https://doi.org/10.1016/j.xphs.2025.103770

3 Pardeike, J., Weber, S., Haber, T., Wagner, J., Zarfl, H. P., Plank, H., & Zimmer, A. (2011). Development of an itraconazole-loaded nanostructured lipid carrier (NLC) formulation for pulmonary application. *International Journal of Pharmaceutics*, *419*(1–2), 329–338. https://doi.org/10.1016/j.ijpharm.2011.07.040

4 Osborn, M. R., Zuniga-Moya, J. C., Mazi, P. B., Rauseo, A. M., & Spec, A. (2025). Side effects associated with itraconazole therapy. *The Journal of Antimicrobial Chemotherapy*, *80*(2), 503–508. https://doi.org/10.1093/jac/dkae437

5 Cheng, Y., Xu, Z., Ma, M., & Xu, T. (2008). Dendrimers as drug carriers: Applications in different routes of drug administration. *Journal of Pharmaceutical Sciences*, *97*(1), 123–143. https://doi.org/10.1002/jps.21079

6 Hu, L., Tang, X., & Cui, F. (2004). Solid lipid nanoparticles (SLNs) to improve oral bioavailability of poorly soluble drugs. *The Journal of Pharmacy and Pharmacology*, *56*(12), 1527–1535. https://doi.org/10.1211/0022357044959

7 Xie, S., Zhu, L., Dong, Z., Wang, Y., Wang, X., & Zhou, W. (2011). Preparation and evaluation of ofloxacin-loaded palmitic acid solid lipid nanoparticles. *International Journal of Nanomedicine*, *6*, 547–555. https://doi.org/10.2147/IJN.S17083

8 Severino, P., Andreani, T., Macedo, A. S., Fangueiro, J. F., Santana, M. H. A., Silva, A. M., & Souto, E. B. (2012). Current State-of-Art and New Trends on Lipid Nanoparticles (SLN and NLC) for Oral Drug Delivery. *Journal of Drug Delivery*, *2012*, 750891. https://doi.org/10.1155/2012/750891

9 Dattani, S., Li, X., Lampa, C., Lechuga-Ballesteros, D., Barriscale, A., Damadzadeh, B., & Jasti, B. R. (2023). A comparative study on micelles, liposomes and solid lipid nanoparticles for paclitaxel delivery. *International Journal of Pharmaceutics*, *631*, 122464. https://doi.org/10.1016/j.ijpharm.2022.122464

10 Wissing, S. A., & Müller, R. H. (2003). The influence of solid lipid nanoparticles on skin hydration and viscoelasticity — *In vivo* study. *European Journal of Pharmaceutics and Biopharmaceutics: Official Journal of Arbeitsgemeinschaft Fur Pharmazeutische Verfahrenstechnik e.V*, *56*(1), 67–72. https://doi.org/10.1016/s0939-6411(03)00040-7

11 Kumar, N., & Goindi, S. (2021). Development and Optimization of Itraconazole-Loaded Solid Lipid Nanoparticles for Topical Administration Using High Shear Homogenization Process by Design of Experiments: *In Vitro*, *Ex Vivo* and *In Vivo* Evaluation. *AAPS PharmSciTech*, *22*(7), 248. https://doi.org/10.1208/s12249-021-02118-3

12 Mukherjee, S., Ray, S., & Thakur, R. S. (2009). Design and evaluation of itraconazole loaded solid lipid nanoparticulate system for improving the antifungal therapy. *Pakistan Journal of Pharmaceutical Sciences*, *22*(2), 131–138.

13 Müller, R. H., Shegokar, R., & Keck, C. M. (2011). 20 years of lipid nanoparticles (SLN and NLC): Present state of development and industrial applications. *Current Drug Discovery Technologies*, *8*(3), 207–227. https://doi.org/10.2174/157016311796799062

14 Mehnert, W., & Mäder, K. (2012). Solid lipid nanoparticles: Production, characterization and applications. *Advanced Drug Delivery Reviews*, *64*, 83–101. https://doi.org/10.1016/j.addr.2012.09.021

15 Mishra, V., Bansal, K. K., Verma, A., Yadav, N., Thakur, S., Sudhakar, K., & Rosenholm, J. M. (2018). Solid Lipid Nanoparticles: Emerging Colloidal Nano Drug Delivery Systems. *Pharmaceutics*, *10*(4), 191. https://doi.org/10.3390/pharmaceutics10040191

16 Cassano, R., Ferrarelli, T., Mauro, M. V., Cavalcanti, P., Picci, N., & Trombino, S. (2016). Preparation, characterization and *in vitro* activities evaluation of solid lipid nanoparticles based on PEG-40 stearate for antifungal drugs vaginal delivery. *Drug Delivery*, *23*(3), 1047–1056. https://doi.org/10.3109/10717544.2014.932862

17 Shah, V., Lesko, L., Fan, J., Fleischer, N., Handerson, J., Malinowski, H., Makary, M., Ouderkirk, L., Roy, S., Sathe, P., Singh, G., Tillman, L., Tsong, Y., & Williams, R. (1997). fDA Guidance for Industry 1 Dissolution Testing of Immediate Release Solid Oral Dosage Forms. *Dissolution Technologies*, *4*, 15–22. https://doi.org/10.14227/DT040497P15

18 Zoubari, G., Staufenbiel, S., Volz, P., Alexiev, U., & Bodmeier, R. (2017). Effect of drug solubility and lipid carrier on drug release from lipid nanoparticles for dermal delivery. *European Journal of Pharmaceutics and Biopharmaceutics: Official Journal of Arbeitsgemeinschaft Fur Pharmazeutische Verfahrenstechnik e.V*, *110*, 39–46. https://doi.org/10.1016/j.ejpb.2016.10.021

19 Gaba, B., Fazil, M., Khan, S., Ali, A., Baboota, S., & Ali, J. (2015). Nanostructured lipid carrier system for topical delivery of terbinafine hydrochloride. *Bulletin of Faculty of Pharmacy, Cairo University*, *53*(2), 147–159. https://doi.org/10.1016/j.bfopcu.2015.10.001

20 Khalil, R. M., Abd El-Bary, A., Kassem, M. A., Ghorab, M. M., & Basha, M. (2013). Influence of formulation parameters on the physicochemical properties of meloxicam-loaded solid lipid nanoparticles. *Egyptian Pharmaceutical Journal*, *12*(1), 63. https://doi.org/10.7123/01.EPJ.0000428643.74323.d9

21 Elmowafy, M., & Al-Sanea, M. M. (2021). Nanostructured lipid carriers (NLCs) as drug delivery platform: Advances in formulation and delivery strategies. *Saudi Pharmaceutical Journal*, *29*(9), 999–1012. https://doi.org/10.1016/j.jsps.2021.07.015

22 Zimmermann, E., & Müller, R. H. (2001). Electrolyte- and pH-stabilities of aqueous solid lipid nanoparticle (SLN^{TM}) dispersions in artificial gastrointestinal media. *European Journal of Pharmaceutics and Biopharmaceutics*, *52*(2), 203–210. https://doi.org/10.1016/S0939-6411(01)00167-9

23 Sanna, V., Gavini, E., Cossu, M., Rassu, G., & Giunchedi, P. (2007). Solid lipid nanoparticles (SLN) as carriers for the topical delivery of econazole nitrate: In-vitro characterization, ex-vivo and in-vivo studies. *The Journal of Pharmacy and Pharmacology*, *59*(8), 1057–1064. https://doi.org/10.1211/jpp.59.8.0002

24 Younus, M., Hawley, A., Boyd, B. J., & Rizwan, S. B. (2018). Bulk and dispersed aqueous behaviour of an endogenous lipid, selachyl alcohol: Effect of Tween 80 and Pluronic F127 on nanostructure. *Colloids and Surfaces. B, Biointerfaces*, *169*, 135–142. https://doi.org/10.1016/j.colsurfb.2018.05.013

25 Karjiban, R. A., Basri, M., Rahman, M. B. A., & Salleh, A. B. (2012). Structural Properties of Nonionic Tween80 Micelle in Water Elucidated by Molecular Dynamics Simulation. *APCBEE Procedia, 2nd International Conference on Chemistry and Chemical Process (ICCCP 2012) May 5-6, 2012*, *3*, 287–297. https://doi.org/10.1016/j.apcbee.2012.06.084

26 Kumar, M., Tiwari, A., Asdaq, S. M. B., Nair, A. B., Bhatt, S., Shinu, P., Al Mouslem, A. K., Jacob, S., Alamri, A. S., Alsanie, W. F., Alhomrani, M., Tiwari, V., Devi, S., Pathania, A., & Sreeharsha, N. (2022). Itraconazole loaded nano-structured lipid carrier for topical ocular delivery: Optimization and evaluation. *Saudi Journal of Biological Sciences*, *29*(1), 1–10. https://doi.org/10.1016/j.sjbs.2021.11.006

27 Ebrahimi, H. A., Javadzadeh, Y., Hamidi, M., & Jalali, M. B. (2015). Repaglinide-loaded solid lipid nanoparticles: Effect of using different surfactants/stabilizers on physicochemical properties of nanoparticles. *Daru: Journal of Faculty of Pharmacy, Tehran University of Medical Sciences*, *23*(1), 46. https://doi.org/10.1186/s40199-015-0128-3

28 Garud, A., Singh, D., & Garud, N. (2012). Solid Lipid Nanoparticles (SLN): Method, Characterization and Applications. *International Current Pharmaceutical Journal*, *1*(11), 384–393. https://doi.org/10.3329/icpj.v1i11.12065

29 Pizzol, C. D., Filippin-Monteiro, F. B., Restrepo, J. A. S., Pittella, F., Silva, A. H., Alves de Souza, P., Machado de Campos, A., & Creczynski-Pasa, T. B. (2014). Influence of Surfactant and Lipid Type on the Physicochemical Properties and Biocompatibility of Solid Lipid Nanoparticles. *International Journal of Environmental Research and Public Health*, *11*(8), 8581–8596. https://doi.org/10.3390/ijerph110808581

30 Mellaerts, R., Mols, R., Jammaer, J. A. G., Aerts, C. A., Annaert, P., Van Humbeeck, J., Van den Mooter, G., Augustijns, P., & Martens, J. A. (2008). Increasing the oral bioavailability of the poorly water soluble drug itraconazole with ordered mesoporous silica. *European Journal of Pharmaceutics and Biopharmaceutics: Official Journal of Arbeitsgemeinschaft Fur Pharmazeutische Verfahrenstechnik e.V*, *69*(1), 223–230. https://doi.org/10.1016/j.ejpb.2007.11.006

31 Mohanty, B., Majumdar, D. K., Mishra, S. K., Panda, A. K., & Patnaik, S. (2015). Development and characterization of itraconazole-loaded solid lipid nanoparticles for ocular delivery. *Pharmaceutical Development and Technology*, *20*(4), 458–464. https://doi.org/10.3109/10837450.2014.882935

32 Pandey, S., Shaikh, F., Gupta, A., Tripathi, P., & Yadav, J. S. (2022). A Recent Update: Solid Lipid Nanoparticles for Effective Drug Delivery. *Advanced Pharmaceutical Bulletin*, *12*(1), 17–33. https://doi.org/10.34172/apb.2022.007

33 Nesseem, D. I. (2001). Formulation and evaluation of itraconazole via liquid crystal for topical delivery system. *Journal of Pharmaceutical and Biomedical Analysis*, *26*(3), 387–399. https://doi.org/10.1016/s0731-7085(01)00414-9

34 Subroto, E., Afifah, T. N., Harlina, P. W., Indiarto, R., Pangawikan, A. D., Huda, S., Wiguna, B., & Geng, F. (2025). Solid lipid nanoparticles of mangosteen peel extract based on monoacylglycerol-diacylglycerol-rich fat and stearic acid: Study on physicochemical properties and encapsulation efficiency. *Future Foods*, *12*, 100719. https://doi.org/10.1016/j.fufo.2025.100719

35 Tao, T., Zhao, Y., Wu, J., & Zhou, B. (2009). Preparation and evaluation of itraconazole dihydrochloride for the solubility and dissolution rate enhancement. *International Journal of Pharmaceutics*, *367*(1–2), 109–114. https://doi.org/10.1016/j.ijpharm.2008.09.034

36 Triboandas, H., Pitt, K., Bezerra, M., Ach-Hubert, D., & Schlindwein, W. (2022). Itraconazole Amorphous Solid Dispersion Tablets: Formulation and Compaction Process Optimization Using Quality by Design Principles and Tools. *Pharmaceutics*, *14*(11), 2398. https://doi.org/10.3390/pharmaceutics14112398

37 Franken, L. E., Boekema, E. J., & Stuart, M. C. A. (2017). Transmission Electron Microscopy as a Tool for the Characterization of Soft Materials: Application and Interpretation. *Advanced Science*, *4*(5), 1600476. https://doi.org/10.1002/advs.201600476

38 Nogueira, S. S., Samaridou, E., Simon, J., Frank, S., Beck-Broichsitter, M., & Mehta, A. (2024). Analytical techniques for the characterization of nanoparticles for mRNA delivery. *European Journal of Pharmaceutics and Biopharmaceutics*, *198*, 114235. https://doi.org/10.1016/j.ejpb.2024.114235

39 Filippov, S. K., Khusnutdinov, R., Murmiliuk, A., Inam, W., Zakharova, L. Ya., Zhang, H., & Khutoryanskiy, V. V. (2023). Dynamic light scattering and transmission electron microscopy in drug delivery: a roadmap for correct characterization of nanoparticles and interpretation of results. *Materials Horizons*, 10(12), 5354–5370. https://doi.org/10.1039/d3mh00717k

40 Subroto, E., Andoyo, R., Indiarto, R., Wulandari, E., & Wadhiah, E. F. N. (2022). Preparation of Solid Lipid Nanoparticle-Ferrous Sulfate by Double Emulsion Method Based on Fat Rich in Monolaurin and Stearic Acid. *Nanomaterials*, *12*(17), 3054. https://doi.org/10.3390/nano12173054

41 Naseri, N., Valizadeh, H., & Zakeri-Milani, P. (2015). Solid Lipid Nanoparticles and Nanostructured Lipid Carriers: Structure, Preparation and Application. *Advanced Pharmaceutical Bulletin*, *5*(3), 305–313. https://doi.org/10.15171/apb.2015.043

42 Chen, W., Gu, B., Wang, H., Pan, J., Lu, W., & Hou, H. (2008). Development and evaluation of novel itraconazole-loaded intravenous nanoparticles. *International Journal of Pharmaceutics*, *362*(1–2), 133–140. https://doi.org/10.1016/j.ijpharm.2008.05.039

43 Das, S., Ng, W. K., Kanaujia, P., Kim, S., & Tan, R. B. H. (2011). Formulation design, preparation and physicochemical characterizations of solid lipid nanoparticles containing a hydrophobic drug: Effects of process variables. *Colloids and Surfaces. B, Biointerfaces*, *88*(1), 483–489. https://doi.org/10.1016/j.colsurfb.2011.07.036

44 Lang, B., McGinity, J. W., & Williams, R. O. (2014). Dissolution enhancement of itraconazole by hot-melt extrusion alone and the combination of hot-melt extrusion and rapid freezing — Effect of formulation and processing variables. *Molecular Pharmaceutics*, *11*(1), 186–196. https://doi.org/10.1021/mp4003706

45 Salah, E., Abouelfetouh, M. M., Pan, Y., Chen, D., & Xie, S. (2020). Solid lipid nanoparticles for enhanced oral absorption: A review. *Colloids and Surfaces. B, Biointerfaces*, *196*, 111305. https://doi.org/10.1016/j.colsurfb.2020.111305

46 Silva, A. C., González-Mira, E., García, M. L., Egea, M. A., Fonseca, J., Silva, R., Santos, D., Souto, E. B., & Ferreira, D. (2011). Preparation, characterization and biocompatibility studies on risperidone-loaded solid lipid nanoparticles (SLN): High pressure homogenization versus ultrasound. *Colloids and Surfaces. B, Biointerfaces*, *86*(1), 158–165. https://doi.org/10.1016/j.colsurfb.2011.03.035

47 Ghasemiyeh, P., & Mohammadi-Samani, S. (2018). Solid lipid nanoparticles and nanostructured lipid carriers as novel drug delivery systems: Applications, advantages and disadvantages. *Research in Pharmaceutical Sciences*, *13*(4), 288–303. https://doi.org/10.4103/1735-5362.235156

48 Zainol, S., Basri, M., Basri, H. B., Shamsuddin, A. F., Abdul-Gani, S. S., Karjiban, R. A., & Abdul-Malek, E. (2012). Formulation Optimization of a Palm-Based Nanoemulsion System Containing Levodopa. *International Journal of Molecular Sciences*, *13*(10), 13049–13064. https://doi.org/10.3390/ijms131013049

49 Andonova, V., & Peneva, P. (2017). Characterization Methods for Solid Lipid Nanoparticles (SLN) and Nanostructured Lipid Carriers (NLC). *Current Pharmaceutical Design*. https://doi.org/10.2174/1381612823666171115105721

50 Martins, S., Tho, I., Ferreira, D. C., Souto, E. B., & Brandl, M. (2011). Physicochemical properties of lipid nanoparticles: Effect of lipid and surfactant composition. *Drug Development and Industrial Pharmacy*, *37*(7), 815–824. https://doi.org/10.3109/03639045.2010.545414

51 Stahl, M. A., Lüdtke, F. L., Grimaldi, R., Gigante, M. L., & Ribeiro, A. P. B. (2024). Characterization and stability of solid lipid nanoparticles produced from different fully hydrogenated oils. *Food Research International (Ottawa, Ont.)*, *176*, 113821. https://doi.org/10.1016/j.foodres.2023.113821

52 Kawakami, K., Oda, N., Miyoshi, K., Funaki, T., & Ida, Y. (2006). Solubilization behavior of a poorly soluble drug under combined use of surfactants and cosolvents. *European Journal of Pharmaceutical Sciences: Official Journal of the European Federation for Pharmaceutical Sciences*, *28*(1–2), 7–14. https://doi.org/10.1016/j.ejps.2005.11.012

53 Segale, L., Giovannelli, L., Mannina, P., & Pattarino, F. (2015). Formulation and characterization study of itraconazole-loaded microparticles. *Pharmaceutical Development and Technology*, *20*(2), 153–158. https://doi.org/10.3109/10837450.2013.852572

54 Lee, J.-H., Park, C., Weon, K.-Y., Kang, C.-Y., Lee, B.-J., & Park, J.-B. (2021). Improved Bioavailability of Poorly Water-Soluble Drug by Targeting Increased Absorption through Solubility Enhancement and Precipitation Inhibition. *Pharmaceuticals (Basel, Switzerland)*, *14*(12), 1255. https://doi.org/10.3390/ph14121255

55 Parikh, T., Sandhu, H. K., Talele, T. T., & Serajuddin, A. T. M. (2016). Characterization of Solid Dispersion of Itraconazole Prepared by Solubilization in Concentrated Aqueous Solutions of Weak Organic Acids and Drying. *Pharmaceutical Research*, *33*(6), 1456–1471. https://doi.org/10.1007/s11095-016-1890-8

56 Kim, J.-K., Park, J.-S., & Kim, C.-K. (2010). Development of a binary lipid nanoparticles formulation of itraconazole for parenteral administration and controlled release. *International Journal of Pharmaceutics*, *383*(1–2), 209–215. https://doi.org/10.1016/j.ijpharm.2009.09.008

57 Khan, J., Rades, T., & Boyd, B. J. (2016). Lipid-Based Formulations Can Enable the Model Poorly Water-Soluble Weakly Basic Drug Cinnarizine To Precipitate in an Amorphous-Salt Form During In Vitro Digestion. *Molecular Pharmaceutics*, *13*(11), 3783–3793. https://doi.org/10.1021/acs.molpharmaceut.6b00594

58 Das, S., & Chaudhury, A. (2011). Recent advances in lipid nanoparticle formulations with solid matrix for oral drug delivery. *AAPS PharmSciTech*, *12*(1), 62–76. https://doi.org/10.1208/s12249-010-9563-0